Thickness Dependence of Oxygen Vacancy Ordering in Strained LaCoO$_{3-x}$ Thin Films

Supporting Information

Ningbin Zhang,[†,‡] Xianhui Tian,[†,‡] Yinlian Zhu,[†] Yujia Wang,[†] Yunlong Tang,[†] Minjie Zou,[†,‡] Jinyuan Ma,[†, //] Yanpeng Feng,[†, #] Wanrong Geng,[†,‡] Yi Cao,[†,‡] and Xiuliang Ma[†, //*]*

[†]Shenyang National Laboratory for Materials Science, Institute of Metal Research, Chinese Academy of Sciences, Wenhua Road 72, 110016 Shenyang, China

[‡]School of Material Science and Engineering, University of Science and Technology of China, Hefei 230026, China

[//]State Key Lab of Advanced Processing and Recycling on Non-ferrous Metals, Lanzhou University of Technology, Langongping Road 287, 730050 Lanzhou, China

[#]University of Chinese Academy of Sciences, Yuquan Road 19, 100049 Beijing, China

[*]Correspondence authors:

E-mail address: ylzhu@imr.ac.cn (Yinlian Zhu)

or xlma@imr.ac.cn (Xiuliang Ma)

This file includes:

1. Low-magnification HAADF images of LCO films with various thickness grown on STO substrate.

2. Strain state analysis of LCO films grown on STO substrates.

3. Table with all peak and trough lattice parameters of LCO grown on various substrates.

4. Low-magnification HAADF images of LCO films with various thickness grown on NGO substrate.

5. Strain state analysis of LCO films grown on NGO substrates.

6. Eight different surface slab models.

7. Table about Calculated cleavage, relaxation and surface energies of the eight slab models of $La_3Co_3O_8$.

1. Low-magnification HAADF images of LCO films with various thickness grown on STO substrate

In the 30 nm thick LCO film (Figure S1a), a large number of dark stripes can be observed to appear perpendicular to the interface. When the thickness of the film is reduced to 14 nm (Figure S1b), it can be noticed that the dark stripes were still vertically arranged perpendicular to the interface, but the density of stripes was significantly reduced compared with that in Figure S1a. When the thickness of the film is further reduced to 5 nm, we see while dark stripes perpendicular to the interface still appear in one region (Figure S1c), stripes parallel to the interface can be identified in another region (Figure S1d). When the thickness of the film was reduced to 3 nm, it is noted that the dark stripes were mainly parallel to the interface (Figure S1e).
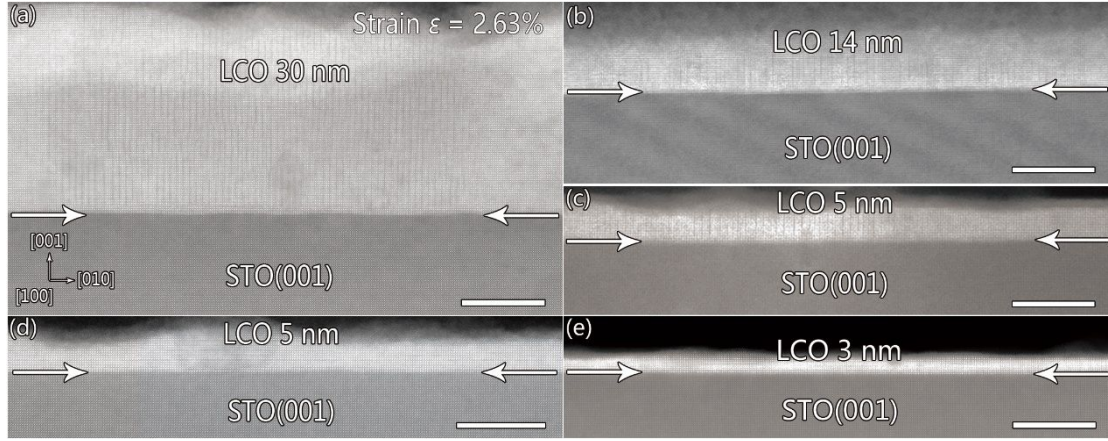
Figure S1. Low-magnification HAADF images of 30 nm (a), 14 nm (b), 5 nm (c), 5 nm (d), 3 nm (e) thick LCO films grown on STO substrate, respectively. To show spatial distribution of oxygen vacancies more clearly in larger areas, two images were stitched together in (d). Scale bar = 15 nm.

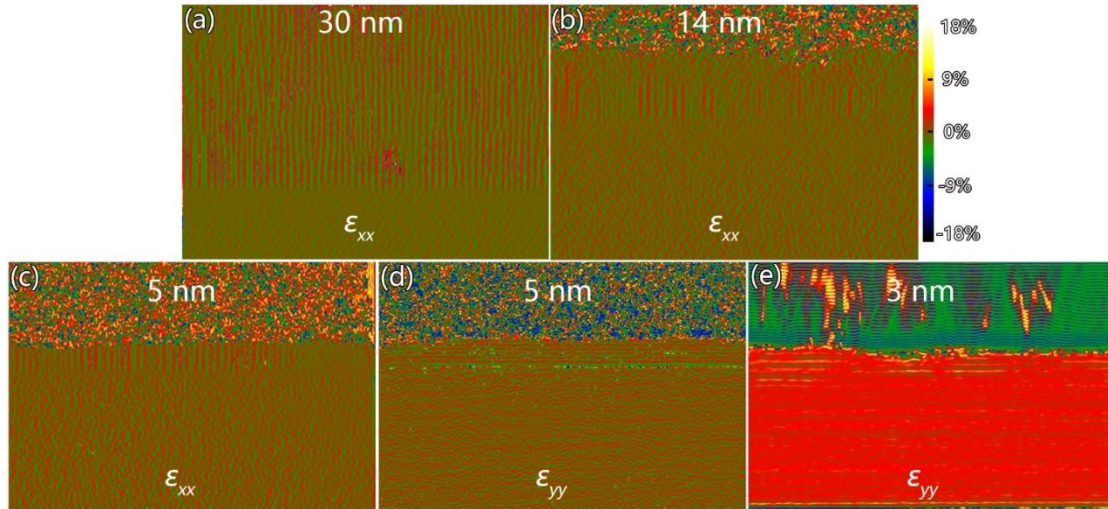## 2. Strain state analysis of LCO films grown on STO substrates.

Figure S2. Strain state analysis of 30 nm (a), 14 nm (b), 5 nm (c), 5 nm (d), and 3 nm (e) LCO/STO films shown in Figure 1a-e, respectively. (a, b, c) are in-plane strain (ε_{xx}) maps, (d, e) are out-of-plane strain (ε_{yy}) maps.

3. Table with all peak and trough lattice parameters of LCO grown on various substrates.

Table S1. Peak and Trough Lattice Parameters of LCO Grown on Various Substrates

LCO/STO Film systems	Peak values(nm)	Trough values(nm)	LCO/NGO Film systems	Peak values(nm)	Trough values(nm)
30 nm	0.44	0.365	30 nm	0.44	0.37
14 nm	0.42	0.38	13 nm	0.43	0.365
5 nm	0.43	0.37	13 nm	0.44	0.36
5 nm	0.45	0.37	10 nm	0.40	0.37
3 nm	0.45	0.35	10 nm (10^{-6} Torr)	0.45	0.37

4. Low-magnification HAADF images of LCO films with various thickness grown on NGO substrate.

From Figure S2a, we can see that in the 30 nm LCO film, the dark stripes were arranged perpendicular to the heterogeneous interface. Compared with Figure S1a, the dark stripe density is significantly reduced, and the stripe distribution is inhomogeneous. For a 13 nm thick LCO film, as shown in Figure S2b, we see that the film was configured with a mixture of vertical and horizontal stripes. It can be seen that the LCO films grown on NGO substrates have undergone a structural evolution when the thickness is reduced to 13 nm. When the thickness is reduced to 10 nm, as shown in Figure S2c, no dark stripe contrast is observed in the whole region. It can be seen that the oxygen vacancy concentration decreases sharply when the thickness decreases. In order to observe the configuration of oxygen vacancies in ultrathin films, we adopted the growth method of reducing annealing oxygen partial pressure to increase the oxygen vacancy concentration, as shown in Figure S2d. Under the annealing oxygen pressure of 10^{-6} Torr, the whole film was mainly stacked with dark stripes along out-of-plane
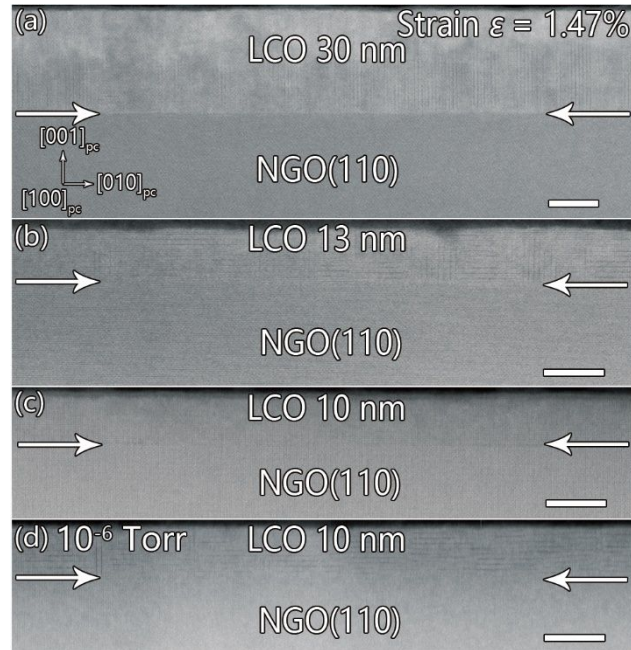
direction.

Figure S3. Low-magnification HAADF images of 30 nm (a), 13 nm (b), 10 nm (c), 10 nm (d) thick LCO films grown on NGO substrates, respectively. (d) was grown under 10^{-6} Torr annealing condition. Scale bar = 15 nm.

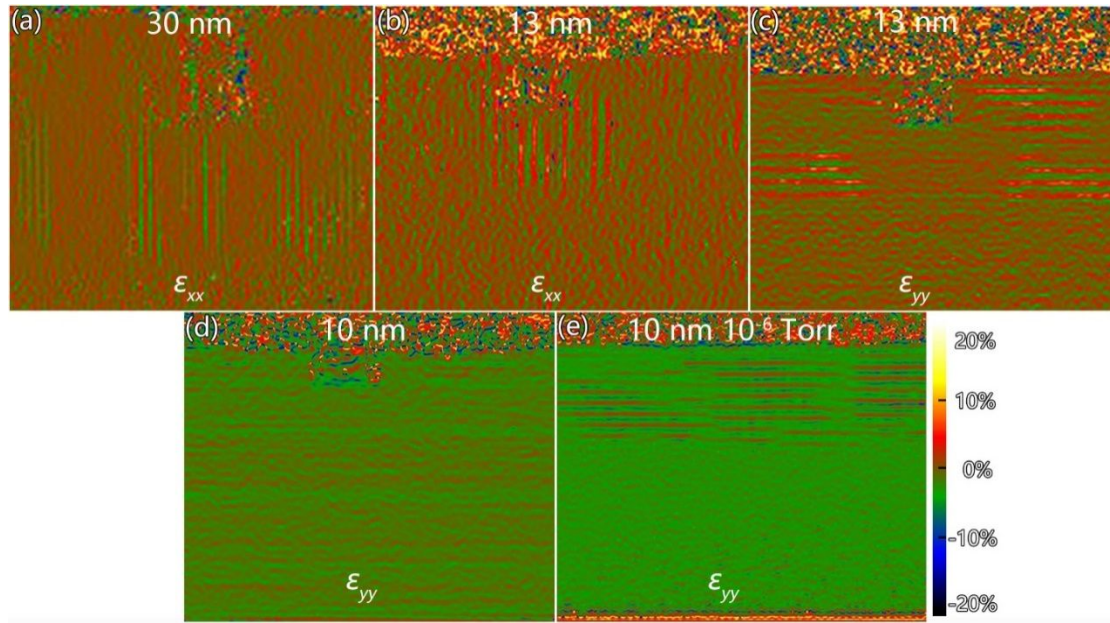**5. Strain state analysis of LCO films grown on NGO substrates.**

Figure S4. Strain state analysis of 30 nm (a), 13 nm (b), 13 nm (c), 10 nm (d), and 10 nm annealed at 10^{-6} Torr (e) LCO/NGO films shown in Figure 3a-d, respectively. (a, b) are in-plane strain (ε_{xx}) maps, (c, d, e) are out-of-plane strain (ε_{yy}) maps.

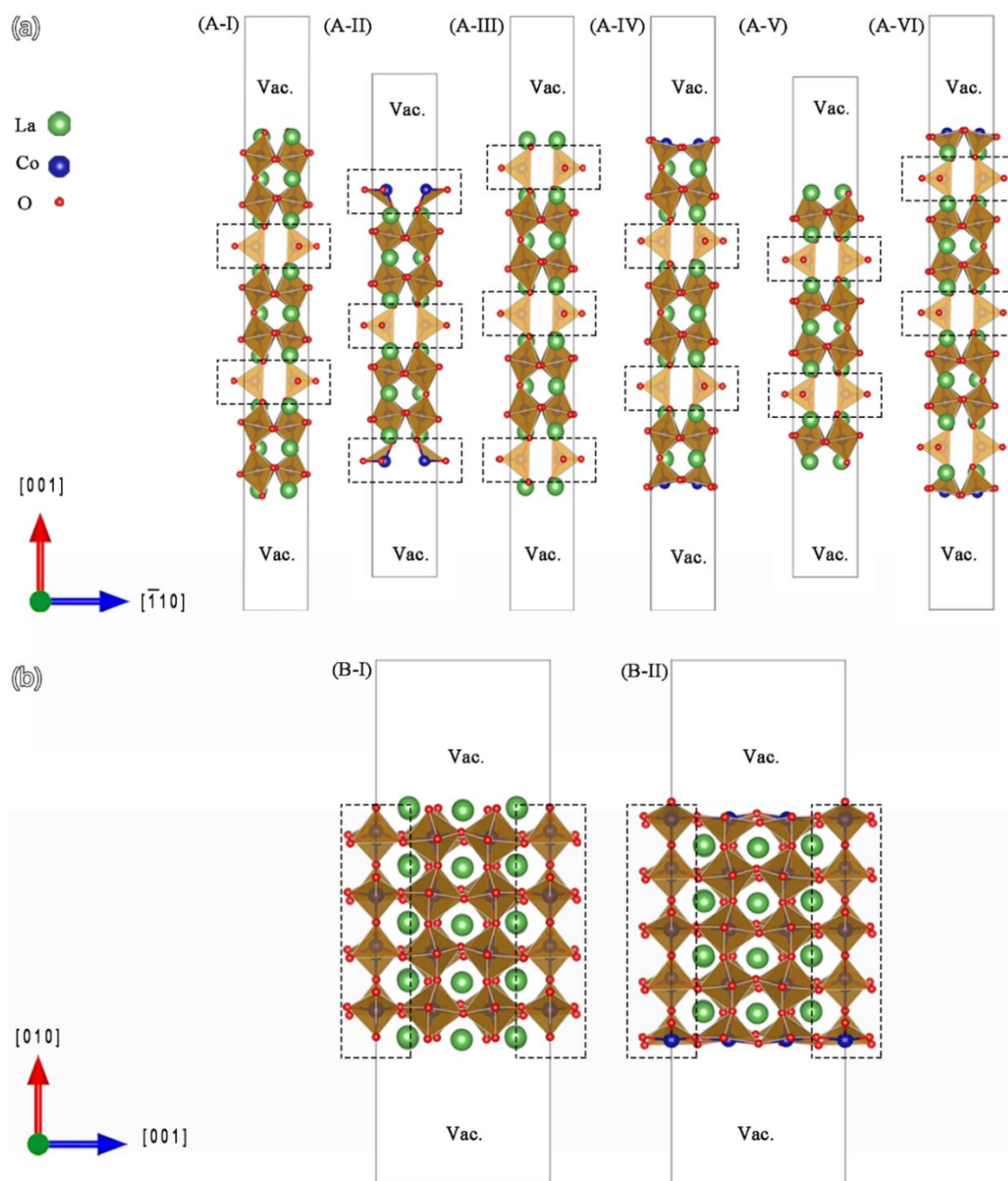**6. Eight different surface slab models.**

Figure S5. Eight different surface slab models. Up panel: the six slab models obtained by three different cleavage of the horizontal bulk model A. Down panel: the two slab models obtained by the cleavage of the vertical bulk model B. The positions of V_O plates are marked with black dashed frame.

7. Table about Calculated cleavage, relaxation and surface energies of the eight

slab models of La$_3$Co$_3$O$_8$.

Table S2 Calculated Cleavage, Relaxation and Surface Energies of the Eight Slab Models of La$_3$Co$_3$O$_8$

Model	E_{cl}/eV·nm^{-2}	E_{rel}/eV·nm^{-2}	E_{surf}/eV·nm^{-2}	E_{surf}/J·m^{-2}
A-I	6.985	-0.855	6.130	0.982
A-II	6.985	-2.566	4.420	0.708
A-III	17.815	-4.089	13.726	2.199
A-IV	17.815	-4.869	12.946	2.074
A-V	11.423	-6.941	4.482	0.718
A-VI	11.423	-4.388	7.035	1.127
B-I	13.121	-5.587	7.534	1.207
B-II	13.121	-5.056	8.065	1.292